

Research on non-stationary characteristics under large-scale multi-antenna vehicle occlusion conditions

Ruihong Zhou¹, Baokang Xiang¹, Kaifeng Huang^{1,*}

¹*School of Mechanical and Electrical Engineering, Huainan Normal University, Huainan, 232038, China*

**Corresponding author: zrh@hnnu.edu.cn*

Keywords: Large-scale multi antenna, Vehicle-to-vehicle communication, Wireless channel measurement

Abstract: The radio wave propagation characteristics of the wireless channel directly affect the transmission rate and transmission quality of the wireless communication system, so it is considered to be the basis of wireless communication system design. The mode of direct communication between vehicles belongs to the low delay sensitive communication type. Channel measurement is carried out under the condition that the link is blocked by other vehicles in the process of vehicle-to-vehicle communication, and the fading characteristics and delay characteristics of vehicle-to-vehicle occlusion are analyzed under different occlusion conditions. Then, a characterization method of channel time non-stationary characteristics in vehicle-to-vehicle communication is proposed, and the relationship between non-stationary characteristics and fading characteristics under vehicle occlusion is analyzed.

1. Introduction

According to the characteristics of large-scale multi-antenna channels, different research teams have selected different wideband multi-antenna channel measurement methods to carry out related research, and analyzed the channel characteristics based on the measurement results. In the literature [1], large-scale multi-antenna channel measurement work was carried out in outdoor campus scenes. A virtual linear array of 128 antennas was used at the transmitting end, and the center carrier frequency was set to 2.6GHz and the bandwidth was set to 50MHz. On this basis, the gain, Rice's scale factor and angular power spectral density of large-scale multi-antenna channels are analyzed. The results of delay expansion are analyzed in the literature [2], and the idea of large-scale multi-antenna channel modeling is discussed in the literature [3]. In the literature [4], large-scale multi-antenna channel measurement was also carried out in outdoor campus scenes at the center carrier frequency of 2.6GHz, and the bandwidth was only 20MHz. However, the virtual array of 112 antennas used at the transmitting end was composed of 7 vertically arranged solid antennas by rotating 16 angles, so the measurement speed was improved to a certain extent. The measurement results in these literature prove that the gains obtained from theoretical analysis in large-scale multi-antenna systems can indeed be realized in actual propagation channels.

The irregular geometric modeling in the car-to-car channel assumes that scatterers are distributed

on both sides of the road and in the road, and sets the area and density of scatterer distribution according to the actual road conditions, thereby establishing a channel model that is closer to the real scene. In the literature [5], the author first proposed the idea of irregular geometric modeling of vehicle-to-vehicle channels in highway scenes, and first extracted the multipath information based on the actual measurement data through the "search-and-elimination" method. Secondly, based on the extraction results, the distribution area and density of different scatterers were modeled, and finally the total impulse response of the channel was obtained by superimposing the impulse responses of the direct path and the primary reflection path. Literature [6] extends the model to campus, urban areas, suburbs and highway scenes based on the literature [5], and doesn't set the scatterer position when modeling diffuse scatterers, but uses a purely random modeling method, and the corresponding modeling formula is given. After that, literature [7-9] made reasonable improvements to the model based on the architecture of irregular geometric modeling, making it more suitable for vehicle-to-vehicle channels under different scene conditions. It should be pointed out that the irregular geometric model takes the time non-stationary characteristics of the vehicle-to-vehicle channel into account in the assumption process, and therefore has become one of the mainstream methods in vehicle-to-vehicle channel modeling.

2. Analysis of non-stationary characteristics of large-scale multi-antennas

The design of wireless channel systems is inseparable from the characterization of the propagation characteristics of wireless channels in relevant environments. Signals transmitted by different antennas at the base station will experience significantly different propagation channels when reaching the user side, resulting in spatial non-stationary characteristics of the channel. From the mathematical analysis, it can be seen that the mean value of the random process of the channel statistical parameters has nothing to do with the distance between the antennas, and the second-order matrix corresponding to the random process is only related to the distance difference between the antennas; from the physical analysis, it can be seen that the channel is at a certain spatial distance. The correlation of one or more time domains or spatial domains exceeds a certain threshold.

The channel parameters of large-scale multi-antennas vary significantly along the antenna dimensions. The intuitive reason for this phenomenon is that the large antenna array size of large-scale multi-antenna systems results in significant changes in the power of the MPC along the antenna dimension, and even the birth and death of the MPC under certain conditions. Therefore, parameters of different dimensions in large-scale multi-antenna channels will experience more significant spatial fluctuations, which is also different from traditional antenna channels and brings new challenges to large-scale multi-antenna channel modeling. From the perspective of physical propagation, each scatterer is not always visible to the entire antenna array, which creates spatial non-stationary characteristics.

SAGE is currently a mainstream algorithm for extracting multipath parameters. The baseband channel impulse response of a large-scale multi-antenna system is shown in equation (1):

$$\mathbf{h}(\tau) = \sum_{l=1}^L \alpha_l e^{-j2\pi f_c \tau_l} \mathbf{P}_2(\varphi_2, l) \mathbf{P}_1(\varphi_1, l)^T \delta(\tau - \tau_l) \cdot \delta(\varphi_1 - \varphi_{1,l}) \cdot \delta(\varphi_2 - \varphi_{2,l}) \quad (1)$$

Among them, α_l , τ_l , $\varphi_{1,l}$ and $\varphi_{2,l}$ are respectively the complex amplitude, delay, departure angle and arrival angle of the l -th MPC under the condition that the carrier frequency is f_c , and vectors $\mathbf{P}_1(\varphi_1, l)$ and $\mathbf{P}_2(\varphi_2, l)$ are both column vectors, representing the channel response of the l -th MPC propagated from the directions $\varphi_{1,l}$ and $\varphi_{2,l}$ respectively. Under the assumption of plane waves,

the equations (2) and (3) of vectors $\mathbf{P}_1(\varphi_1, l)$ and $\mathbf{P}_2(\varphi_2, l)$ are as follows:

$$\mathbf{P}_1(\varphi_1, l) = [1, e^{-j\frac{2\pi d \sin \varphi_{1,l}}{\lambda}}, \dots, e^{-j\frac{2\pi W d \sin \varphi_{1,l}}{\lambda}}]^T \quad (2)$$

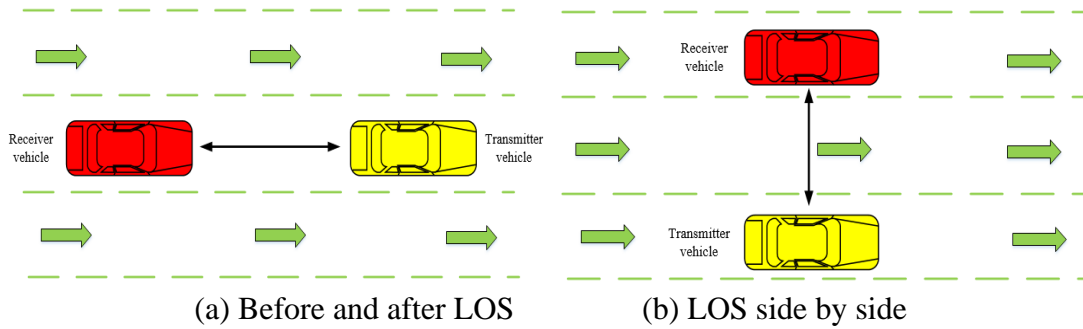
$$\mathbf{P}_2(\varphi_2, l) = [1, e^{-j\frac{2\pi d \sin \varphi_{2,l}}{\lambda}}, \dots, e^{-j\frac{2\pi N_{R_x} d \sin \varphi_{2,l}}{\lambda}}]^T \quad (3)$$

Among them, W represents the size of the spatial sliding window of the emission antenna array to estimate the parameter space. D represents the interval between the launch antenna array and the receiving antenna array adjacent antenna, and $d = \lambda/2$, and λ represents the wavelength of the wavelength. In the process of estimating the parameters, the union maximum function of each parameter needs to be obtained from their maximum likelihood estimation. In order to reduce the complexity, the SAGE algorithm uses iteration to update parameters to obtain the maximum like - like estimation of all vectors under the set conditions. During each iteration process, the two strategies can be used with serial interference to eliminate and parallel interference to eliminate the two strategies to treat the observation set during the expectation process.

During each iteration of the standard SAGE algorithm, using the SIC method needs to delete the estimated LPC from the observation data, and the estimated process will continue in the remaining data, which will easily cause the estimation of the same delay of the same delay. The MPC causes the same communication distance in different directions or scattering diameters. By improving the SAGE algorithm by adding a noise power retriever to each estimated multi -diameter delay position. If the difference between the existing estimated multi-diameter delay position is estimated to be less than the noise power limit between the power of the power of the MPC and the power measurement data of the corresponding location, the position of the multi -diameter delay will be delete.

3. Multi-antenna channel measurement in vehicle-to-vehicle communication scenarios

The typical scenes of vehicles include urban areas, suburbs, highways, rural areas, etc., and these typical scenes will also become the main scenario of vehicle-to-vehicle communication systems. Different from the traditional via camera assisted, LOS and NLOS conditions are differentiated. The channels of this article have been measured on the channels of LOS and NLOS under vehicle cover conditions. Because the relative positions between vehicles and vehicles are diverse in the actual vehicle communication process of vehicles, we have considered a variety of different ways of driving in measurement. As shown in Figure 1, there are three lanes in urban roads and telling highways. In such a three-lane road, the measurement has been considered four methods.



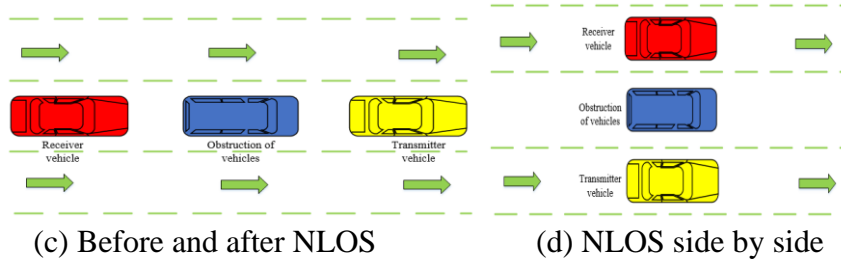


Figure 1: Measurement method of highway scene

Method 1 is the case where the launch vehicle is launched in front of the receiver vehicle under the LOS conditions, and referred to as the "front and rear" method of LOS, This method will be used as an unobstructed reference method. Method 2 is the occlusion mode corresponding to the LOS before and after mode, where the occlusion vehicle is located between the launching locomotive vehicle and the receiver vehicle, and this method is referred to as the "NLOS before and after" mode. Method 3 is the case where the transmitter vehicle is launched side by side under the LOS conditions, and is referred to as the "LOS side by side" method, and the launch vehicle and the receiving vehicle are driving on the inner side and the outermost lanes, respectively. Method 4 is the corresponding obstruction method of the LOS side by side. Among them, the blocking vehicle is located on the middle lane between the launch vehicle and the receiving vehicle. This method is referred to as the "NLOS side by side". In LOS before and after mode and NLOS before and after mode, all vehicles are driving in the same direction of the middle lane, and keep the speed of the vehicle is basically the same. The distance between the transmitter vehicle and the receiver vehicle is kept in the same fluctuation range, the error is not more than 5 m. It should be noted that the relative position between vehicles during the measurement process cannot be kept fixed due to complex traffic conditions. In LOS side by side and NLOS side by side, all vehicles are traveling in different lanes in the same direction, and the vehicles are kept side by side and at roughly the same speed.

During the measurement, data collection under LOS and NLOS conditions is carried out separately along the same road. Although it is not completely accurate, based on the observation of speed and observation of speed and obstruction, the distance between the transmitting vehicle and the receiving vehicle under different conditions of the measurement period fluctuates within a few meters. When the value of path loss of about 2 and the communication distance is no more than 15 m, the measured power change will be on the order of 1dB or less. The reason for adopting this measurement method is to evaluate the impact of different occluding vehicles on the channel. In addition, the channel measurement of the vehicle to the vehicle in this article is only applicable to a smaller communication distance range, and if the distance between the receiving antenna is far more than the distance between the measurement, the result will not be applicable. For example, when the distance between the transceiver antenna is very small (the distance between the transmitter vehicle and the shielding vehicle and the shielding vehicle and the receiver vehicle is in the order of centimeters) or the distance between the transceiver antenna is very large (the distance between the transmitter vehicle and the receiver vehicle is in the order of kilometers), the corresponding channel measurement needs to be carried out and reasonable results can be obtained.

At the receiving end, the receiver collects the amplitude and phase of the complex channel impulse response, and the number of channel impulse responses collected under different conditions does not exceed 1500, and the expression of time-varying impulse response at each moment can be expressed by the superposition of $N(t)$ MPC impulse responses, as shown in equation (4).

$$h(t, \tau) = \sum_{i=1}^{N(t)} \alpha_i(t) e^{-j\phi_i(t)} \delta(\tau - \tau_i(t)) \quad (4)$$

Where $\alpha_i(t)$, $\phi_i(t)$ and $\tau_i(t)$ represent the amplitude, phase, and delay of Article i MPC at time t, respectively, while N(t) represents the number of MPCs active at time t. The time-varying PDP is therefore expressed as equation (5).

$$P(t, \tau) = |h(t, \tau)|^2 \quad (5)$$

At a fixed time, the RMS delay extension can be calculated by the PDP of the time, the expression of which is shown in equation (6).

$$\sigma_\tau = \sqrt{\frac{\int_0^\infty \tau^2 P(\tau) d\tau}{\int_0^\infty P(\tau) d\tau} - \bar{\tau}^2} \quad (6)$$

Among them, $\bar{\tau}$ represents an average delay, and its expression is as shown in the equation (7):

$$\bar{\tau} = \frac{\int_0^\infty \tau P(\tau) d(\tau)}{\int_0^\infty P(\tau) d(\tau)} \quad (7)$$

In the process of calculating the RMS delay expansion, the MPC with a peak power difference between the power and peak power in each PDP will be deleted to obtain effective MPCs in the channel. Each time the receiving power can be obtained by responding to the power of MPC in response time PDP. Assuming that the receiving power under the LOS conditions is P_{r0} , and the receiving power under the NLOS conditions corresponding to it is P_{r1} , the vehicle loss at every time can be expressed as equation (8).

$$P_{r0} - P_{r1} \quad (8)$$

According to equation (8), vehicle loss parameter S can be obtained by subtracting the received power at different times under LOS and NLOS conditions. Therefore, with the received power obtained under LOS conditions in urban areas as a reference, the statistical histogram of the slave vehicle loss parameter S obtained under NLOS conditions in four urban areas is shown in Figure 2. Gaussian distribution was used to fit statistical histograms under different conditions, and the fitting curves of parameter S in the logarithmic domain were marked in Figure 2. Except NLOS side-by-side method, Gaussian fitting of parameter S in other methods can be verified by KS criterion with 95% confidence, thus verifying the accuracy of fitting. According to the results in Figure 2, a phenomenon can be observed: there is a significant difference in vehicle loss between the NLOS and NLOS side by side modes, and the mean value of vehicle loss in NLOS side by side mode is smaller than the corresponding value before and after NLOS.

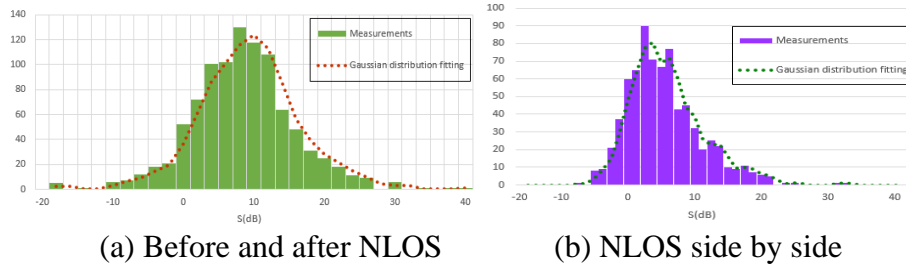


Figure 2: Statistical histogram of vehicle occlusion loss

The statistical values of vehicle wear and tear are shown in Table 1, including the measured median and 90% quantile values as well as the Gaussian fitting mean and standard deviation.

Table 1: Statistical table of vehicle wear and tear

Vehicle loss S (dB)	Measurement parameters		Gaussian fitting parameters	
	median	90% percentile value	mean value	standard deviation
Before and after NLOS	7.92	16.58	8.34	7.12
NLOS side by side	5.93	14.26	6.82	5.74

According to the measured median value of vehicle loss in the table, it can be found that the value of urban NLOS before and after the condition is 7.92 dB, while the value of urban NLOS under the condition of urban NLOS side by side is only 5.93 dB. Therefore, in the urban scene, the loss of vehicles in front and back mode is greater than that in side by side mode. The distance between sending and receiving antennas in side by side mode is much smaller than that between sending and receiving antennas in front and back mode. Under the condition of using the same occlusion vehicle, the area and shape of the occlusion are significantly different due to the relative position of different vehicles, which results in different multipath propagation characteristics of the signal. Due to the difference in the relative position of the vehicle to the surrounding environment during driving, the composition of the receiving MPC will also be different. Based on the calculation of vehicle occlusion fading loss under different conditions, the vehicle loss is analyzed by Gaussian distribution.

4. Conclusion

In this paper, the fading characteristics and time non-stationary characteristics of vehicle-to-vehicle channel are studied under the condition of vehicle-to-vehicle moving forward and side by side. Based on SAGE algorithm, the multi-path parameters of the channel are obtained, and the non-stationary characteristics of the large-scale multi-antenna channel are validated and preliminarily defined. Based on the channel measurement of highway scenes in the urban area, the vehicle blocking losses of vehicles under the relative position conditions of different vehicles were extracted, and the causes of the non-smooth characteristics of time were analyzed in depth, and the relationship between the stable distance and the vehicle loss was found. Methods to carry out measurement of LOS and NLOS conditions separately, accurately locate the decline characteristics under different conditions. There is a significant difference between vehicle loss before and after the NLOS side by side, and the average value of the NLOS side by side is less than the corresponding value before and after the NLOS.

References

- [1] Changzhen Li, Junyi Yu, Wei Chen, Kehao Wang, Kun Yang. *Measurements and analysis of vehicular radio channels in the inland lake bridge area* [J]. *IET Microwaves, Antennas & Propagation*, 2019, 13(9):1394-1401.
- [2] Xiongwen Zhao, Qi Wang, Shu Li, Mengjun Wang, Shaohui Sun. *Wideband Millimeter-Wave Channel Characterization Based on LOS Measurements in an Open Office at 26GHz*. *IEEE Vtc Spring IEEE*, 2016.
- [3] Kim Taehyoung, Min Kyungsik, Park Sangjoon. *Self-Interference Channel Training for Full-Duplex Massive MIMO Systems* [J]. *Sensors*, 2021, 21(9): 3250-3263.
- [4] Pang Yucui, Xiao Yuhan, Liu Song, He Yun. *Solving Manifold Ambiguity by Sliding the Array in MIMO Radar* [J]. *Journal of Physics: Conference Series*, 2021, 1944(1):654-668.
- [5] Dwivedi Ajay Kumar, Sharma Anand, Singh Ashutosh Kumar, Singh Vivek. *Metamaterial inspired dielectric resonator MIMO antenna for isolation enhancement and linear to circular polarization of waves* [J]. *Measurement*, 2021, 182(03):637-648.
- [6] Li Min, Wang Xin, Mao Pandi. *Noise Reduction of Composite Digital Array Antenna with on 5GHz Wireless Band* [J]. *Computer Simulation*, 2020, 37(05):119-123.
- [7] Chen Z, Huan X, Yang W, et al. *A low-profile dual-band multimode patch antenna for wireless local area network and cellular vehicle-to-everything communications* [J]. *International Journal of RF and Microwave Computer-Aided Engineering*, 2021, 31(12).
- [8] He R, Ai B. *Wireless Channel Measurement and Modeling in Mobile Communication Scenario: Theory and Application* [M]. *CRC Press*: 2023-08-08.
- [9] Mao Jingmin, Wei Zaixue, Xing Bingqian, Liu Kaizhen, Zhao Yi. *In Urban Environment Vehicle-to-Vehicle Channel Modeling Based on Geometric Random Model* [J]. *Journal of Beijing University of Posts and Telecommunications*, 2021, 44(02):124-130.